J. Phys.: Condens. Matter **9** (1997) 4345–4364. Printed in the UK PII: S0953-8984(97)81908-X

Tight-binding molecular dynamics simulations of semiconductor alloys: clusters, surfaces, and defects

Y P Feng†, C K Ong†, H C Poon† and D Tománek‡

† Department of Physics, National University of Singapore, Singapore 119260

‡ Department of Physics and Astronomy, Michigan State University, East Lansing, MI 48824-1116, USA

Received 17 February 1997, in final form 3 April 1997

Abstract. We extend the tight-binding molecular dynamics technique to simulations of III–V semiconductor alloy clusters, surfaces, and defects. The total energy of the alloy system is calculated using a newly developed tight-binding parametrization of *ab initio* band structures of bulk alloys and their pure components, for different structures and lattice parameters. The non-local binding in the lattice is compensated by pairwise repulsion to reproduce the *ab initio* total energies. Molecular dynamics techniques are incorporated into the tight-binding total energy scheme following the prescription of Khan and Broughton (Khan F S and Broughton J Q 1989 *Phys. Rev.* B **39** 8592). The method is used to study small Ga_mAs_n clusters, the GaAs(110) surface, and an As vacancy in bulk GaAs. Good agreement with previous studies and available experimental results is obtained in each case.

1. Introduction

Since its introduction nearly thirty years ago, the density functional formalism [1] has established itself as the method of choice for predictive calculations of solids. It has been widely used in studies of structural, electronic, and dynamical properties of various materials. The method, however, is computationally very demanding and applicable to relatively small systems only, typically up to a few tens of atoms. In order to perform 'quantum mechanical' molecular dynamics simulations for larger systems, other simpler approaches, such as the tight-binding approximation, have been proposed to determine the electronic binding. The resulting tight-binding molecular dynamics (TBMD) has been proven to be one of the most useful theoretical tools in probing the microscopic properties of semiconductors. It has successfully predicted and explained a wide range of properties of elemental semiconductors such as Si and C [2–11]. However, due to the complexity introduced with polar bonds and charge-transfer effects in heterovalent compounds, applications of TBMD to semiconductor alloy systems are still scarce. Molteni *et al* [12] have proposed a TBMD scheme for III–V semiconductors. In this scheme, a simple interpolative method is used to reproduce the cohesion energy phase diagram of GaAs. The model has been used to simulate the structures of amorphous and liquid GaAs, as well as point defects in GaAs with relatively good success [12–16]. In this paper, we present an alternative approach to the tight-binding total energy calculation that is based on full parametrization of *ab initio* band structures. The *ab initio* density functional theory within the local density approximation (LDA) [1] is used to determine the electronic structure and the total energy of bulk Al, As, and Ga in the face-centred cubic (fcc) and diamond phases, the stoichiometric AlAs and GaAs alloys in

0953-8984/97/214345+20$19.50

the zinc-blende structure, as well as the isolated atoms. The hopping integrals, which appear in the tight-binding scheme, are obtained by fitting the band structure and total energy in the tight-binding scheme to those of the LDA calculations, for different structures and lattice parameters. The non-local attraction in the lattice is compensated by pairwise repulsive energies to reproduce the *ab initio* total energy data. This scheme, therefore, is expected to yield better agreement with *ab initio* total energy than the model proposed by Molteni *et al* [12].

The scheme is used to determine structural and electronic properties of GaAs and AlAs systems. In this study, we are particularly interested in small clusters, surfaces of these alloys, and defects in the bulk. In addition to providing further theoretical understanding of the properties of the systems concerned, these calculations will be used to assess the validity of the semiempirical, bulk-fitted, tight-binding total energy scheme in describing structures with low symmetry and hence the transferability of the parameters.

The paper is organized as follows. The tight-binding total energy formalism is described in the next section, followed by our tight-binding parametrization and the molecular dynamics technique. In the remaining sections, we present our simulation results for the (110) surface of GaAs, an As vacancy in GaAs, and small Ga_mAs_n clusters.

2. Tight-binding total energy formalism

Consider a semiconductor alloy system consisting of N atoms. The total energy of the system is written as [3, 4]

$$E = \sum_{k,n} \epsilon_n(k) + \sum_{l=2}^{N} \sum_{l'=1}^{l-1} E_{rep}(|\boldsymbol{R}_l - \boldsymbol{R}_{l'}|) + U \sum_{l=1}^{N} (q_l - q_l^0)^2 \tag{1}$$

where $\epsilon_n(k)$ is the single-electron band-structure energy, E_{rep} is a pairwise repulsive potential, and $\boldsymbol{R}_l$ is the position of atom l. q_l is the self-consistent charge of atom l, and q_l^0 is 3.0 for a Ga atom and 5.0 for an As atom. The first term in equation (1) is the total band-structure energy. The second term is the total repulsive energy which contains ion–ion repulsion, exchange–correlation energy, and accounts for the double counting of electron–electron interactions in the band-structure energy term. The last 'Hubbard-like' term imposes an energy penalty on large interatomic charge transfers [3]. In agreement with previous studies [3, 4], the results of our calculations are not very sensitive to the value of U and a value around 1 eV is used.

We have used a simple two-centre Slater–Koster parametrization [17] for our four-state (s, p_x, p_y, p_z) nearest-neighbour tight-binding Hamiltonian. The wave functions Ψ_i ($i = 1, 2, \ldots, M$, where M is the number of occupied single-particle states) are expanded in terms of a basis $\{\phi_{l\alpha}\}$ consisting of four orbitals of s, p_x, p_y, and p_z character that are located on each of the N atoms:

$$\Psi_i(\boldsymbol{r}) = \sum_{l=1}^{N} \sum_{\alpha}^{4} c_{l\alpha}^i \phi_{l\alpha}(\boldsymbol{r}) \qquad i = 1, 2, \ldots, M. \tag{2}$$

Using the above wavefunction, the Schrödinger equation of the system is transformed into a matrix equation and the matrix elements depend on the hopping integrals $V_{ss} = \langle \mathrm{sc}|H|\mathrm{sa}\rangle$, $V_{sp\sigma}^{ca} = \langle \mathrm{sc}|H|p_z\mathrm{a}\rangle$, $V_{sp\sigma}^{ac} = \langle \mathrm{sa}|H|\mathrm{p}_z\mathrm{c}\rangle$, $V_{pp\sigma} = \langle \mathrm{p}_z\mathrm{c}|H|\mathrm{p}_z a\rangle$, $V_{pp\pi} = \langle \mathrm{p}_x\mathrm{c}|H|\mathrm{p}_x a\rangle$, and the self-energy terms $E_s^c = \langle \mathrm{sc}|H|\mathrm{sc}\rangle$, $E_p^c = \langle \mathrm{p}_x\mathrm{c}|H|\mathrm{p}_x\mathrm{c}\rangle$, $E_s^a = \langle \mathrm{sa}|H|\mathrm{sa}\rangle$, $E_p^a = \langle \mathrm{p}_x\mathrm{a}|H|\mathrm{p}_x\mathrm{a}\rangle$, where c and a indicate the cation atom and the anion atom respectively, if just the first-nearest-neighbour interaction is considered. These parameters are normally determined by

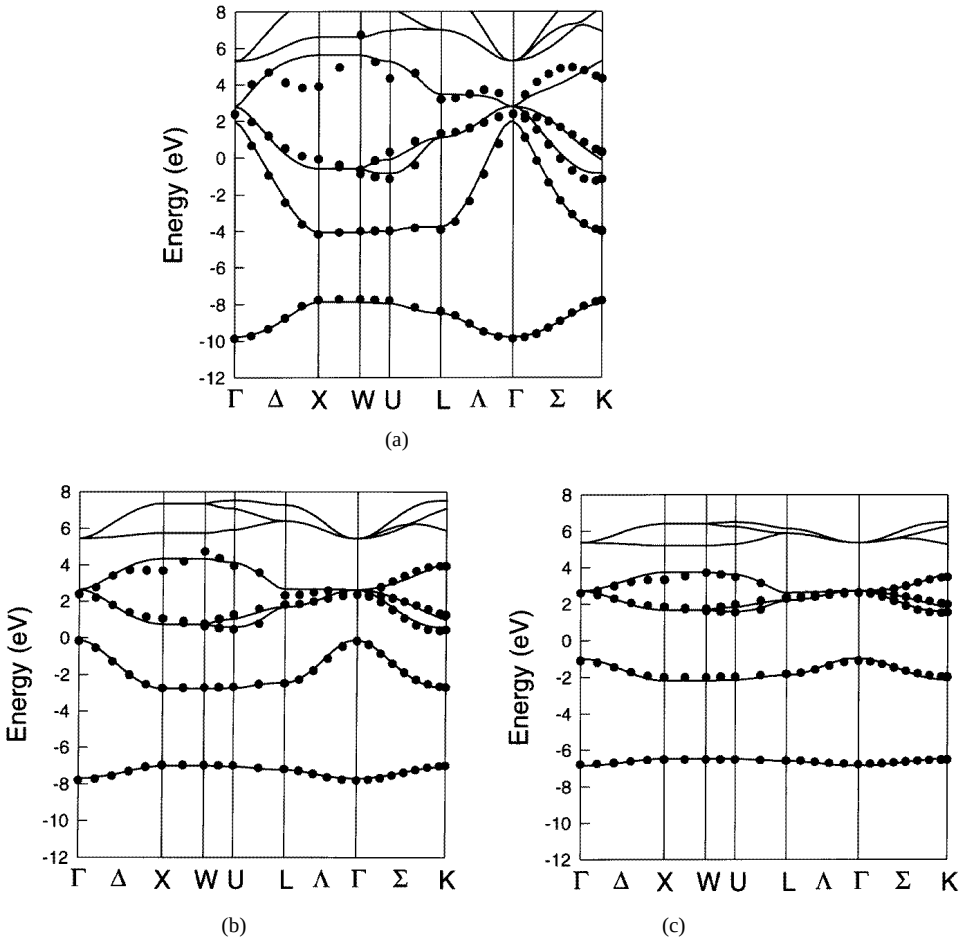

Figure 1. LDA (•) and tight-binding (solid lines) band structures for GaAs in the zinc-blende structure at nearest-neighbour distances of (a) 2.5 Å, (b) 2.9 Å, and (c) 3.3 Å. The Fermi level is set to $E = 0$. The four valence bands and the lowest conduction band have been included in the tight-binding fit.

comparing the calculated band structure with a first-principles or empirically known band structure. Given these parameters, the matrix equation can be solved to obtain the valence and lowest conduction band energies of the system being studied.

In a molecular dynamics simulation, the nearest-neighbour distance and hence the hopping integrals vary as a function of time. A d^{-2} scaling [18] of the hopping integrals at equilibrium interatomic distance has been used in most studies as well as in the tight-binding molecular dynamics (TBMD) method proposed by Molteni *et al* [12]. While such a simple scaling method works well for atomic arrangements close to the equilibrium distance, the reliability of such a scheme is more problematic in the case of large deviations from equilibrium, such as are often encountered in molecular dynamics simulations. In the present study, we fit first-principles band structures for different crystalline structures and interatomic distances using one universal set of parameters. We expect our tight-binding scheme to reproduce the *ab initio* total energy not only for one equilibrium structure, but also in different structures and for varying interatomic distances.

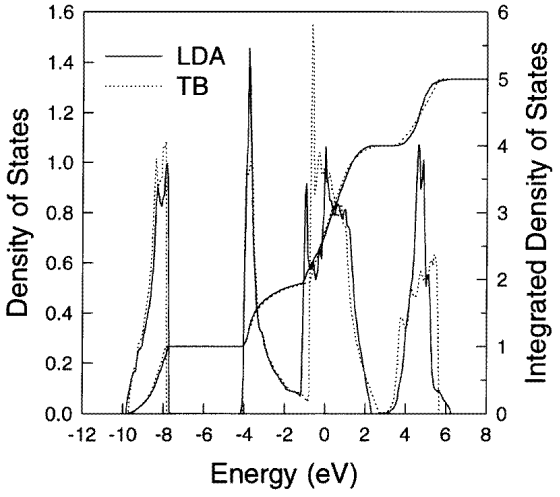

(a)

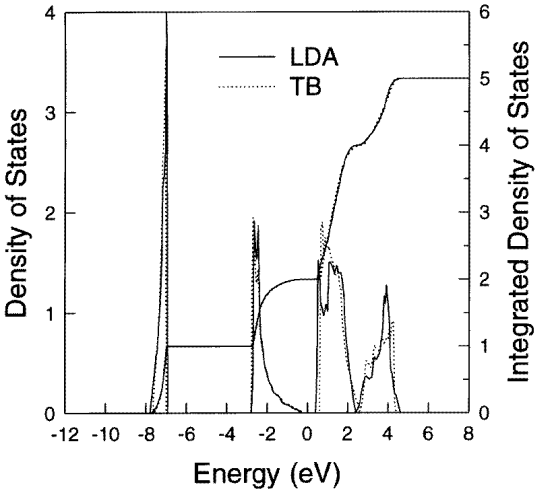

(b)

Figure 2. A comparison between LDA results (solid lines) and tight-binding results (dashed lines) for the density of states and integrated density of states of GaAs in the zinc-blende structure at the nearest-neighbour distances (a) 2.5 Å, (b) 2.9 Å, and (c) 3.3 Å. The Fermi level is set to $E = 0$.

3. Tight-binding parametrization

The *ab initio* band structures and total energies are calculated using the local density functional (LDA) formalism for crystalline GaAs, AlAs, as well as their pure crystalline components. The zinc-blende structure is assumed for GaAs and AlAs, while both diamond and fcc structures are considered for the pure materials Ga, Al, and As. In each case, the LDA band structure and total energy are calculated for a number of different lattice parameters. The hopping integrals are then adjusted to match the band structure and the total energy obtained by LDA for each lattice parameter and each structure. This is done by a

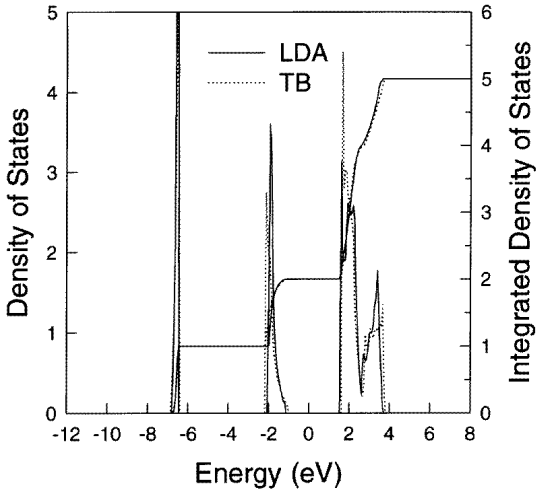

(c)

Figure 2. (Continued)

systematic multidimensional minimization of the weighted differences of the band-structure energy and the energy eigenvalues throughout the Brillouin zone between the tight-binding and the LDA values. Since we are only interested in ground-state properties, emphasis is placed on the occupied and lowest unoccupied states; higher conduction bands are ignored in most of the fitting procedures. All $\boldsymbol{k}$-points in the Brillouin zone are treated equally.

In figure 1, we compare the tight-binding band structures based on our parametrization

Table 1. Self-energies (a) and fitted hopping integrals for Ga in the diamond structure (b); As in the diamond structure (c); and GaAs in the zincblende structure (d). The nearest-neighbour distance (d) is given in Å and the energies are measured in eV.

(a)		E_s	E_p			
	Ga	−2.18	4.36			
	As	−5.622	3.748			
(b)	d	ss_σ	sp_σ	pp_σ	pp_π	
	2.5	−1.5214	1.8707	2.0767	−1.2314	
	2.9	−0.8826	1.1620	1.4855	−0.8139	
	3.3	−0.5130	0.6987	1.0912	−0.5534	
(c)	d	ss_σ	sp_σ	pp_σ	pp_π	
	2.5	−1.1842	1.7325	2.5888	−0.7869	
	2.9	−0.5881	0.9795	1.7104	−0.4643	
	3.3	−0.2822	0.4775	1.0975	−0.2714	
(d)	d	ss_σ	sp_σ^{ca}	sp_σ^{ac}	pp_σ	pp_π
	2.5	−1.4031	1.6601	2.2720	2.6210	−0.8535
	2.9	−0.8424	0.8534	1.7223	1.9905	−0.4805
	3.3	−0.5940	0.0336	1.3051	1.4942	−0.2649

to the LDA results for GaAs, for three different lattice parameters. The corresponding densities of states are shown in figure 2. The same fit quality is also obtained for all of the other systems. The parameters obtained for diamond Ga, diamond As, and zinc-blende GaAs are listed in table 1.

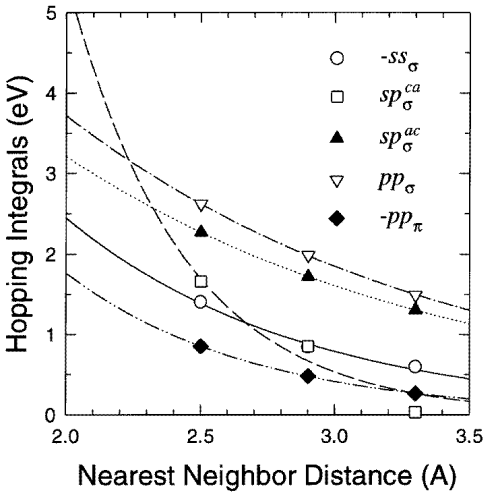

Figure 3. Tight-binding hopping integrals with the functional dependence $V = V_0 \exp(-\beta r)$ (lines) as functions of the interatomic distance for GaAs in the zinc-blende structure. Optimum fits of the LDA band structure at selected nearest-neighbour distances are given by the data points.

Once the tight-binding parameters are determined for a given structure at several lattice parameters, we fit the hopping integrals by a simple exponential function that decreases as a function of the interatomic distance r, so that hopping integrals at any given value of r can be easily interpolated. This type of parametrization provides a more realistic r-dependence of the hopping integrals, and is more accurate than empirical relationships such as the r^{-2}-scaling when describing interactions at interatomic distances that deviate significantly from the equilibrium distance. The present tight-binding parametrization of the *ab initio* band structure at three values of lattice parameters produces sufficient accuracy. Additional fitting at different lattice parameters can be done to increase the accuracy if necessary. The hopping integrals obtained for GaAs in the zinc-blende structure are shown in figure 3. In subsequent calculations, the hopping integrals at any given interatomic distance are interpolated using the simple exponential distance dependence.

Using the interpolated hopping integrals, the tight-binding band-structure energy can be obtained for any geometry and interatomic distance. We then *define* the repulsive energy as the difference between the 'exact' binding energy, obtained using *ab initio* calculations, and the tight-binding band-structure energy, as shown in figure 4 for GaAs in the zinc-blende structure. This is done again for a number of interatomic distances. A simple analytical curve containing up to three exponential functions is then used to represent the repulsive energy as a function of the interatomic distance. The tight-binding scheme therefore closely reproduces the *ab initio* binding energy in the range of interatomic distances considered, and fits exactly the *ab initio* values for the calculated geometries and interatomic distances. The accuracy could be further improved by increasing the number of interatomic distances in the tight-binding parametrization.

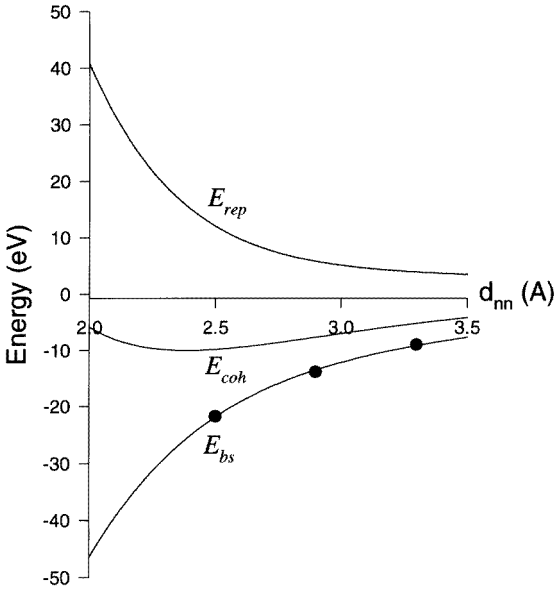

Figure 4. The binding energy (E_{coh}), repulsive energy (E_{rep}), and band-structure energy (E_{bs}) for GaAs in the zinc-blende structure, as functions of the interatomic distance.

4. Molecular dynamics

We employ the molecular dynamics proposed by Car and Parrinello [19] following the prescription of Khan and Broughton [4]. In this procedure, the electronic degrees of freedom $\{c^i_{l\alpha}\}$ are treated as 'position' variables of classical particles of fictitious mass μ. The trajectories associated with the ionic and electronic coordinates are predicted via molecular dynamics, with the forces on the electrons calculated from the 'fictitious Lagrangian'

$$L = \frac{1}{2}\mu \sum_{i,l,\alpha} (\dot{c}^i_{l\alpha})^2 + \frac{1}{2}\sum_l M_l \dot{\boldsymbol{R}}_l^2 - E(\{\boldsymbol{R}_l\}, \{c^i_{l\alpha}\}). \tag{3}$$

Here, l, α and i label atoms, atomic orbitals (s, p_x, p_y, and p_z), and occupied wave functions, respectively. The orthonormality of the occupied states requires the following constraints on $c^i_{l\alpha}$:

$$\sum_{l\alpha} c^i_{l\alpha} c^j_{l\alpha} = \delta_{ij} \tag{4}$$

which lead to the following equations of motion for the ionic and electronic coordinates:

$$M_l \ddot{\boldsymbol{R}}_l = -\frac{\partial}{\partial \boldsymbol{R}_l} E(\{\boldsymbol{R}_l\}, \{c^i_{l\alpha}\}) \tag{5}$$

and

$$\mu \ddot{c}^i_{l\alpha} = -\frac{\partial}{\partial c^i_{l\alpha}} E(\{\boldsymbol{R}_l\}, \{c^i_{l\alpha}\}) + \sum_j \Lambda_{ij} c^j_{l\alpha}. \tag{6}$$

Here, i and j run over the occupied states, and Λ_{ij} is a symmetric matrix whose elements are the Lagrange multipliers given by [4]

$$\Lambda_{ij} = \sum_{l\alpha} \left(\frac{1}{2}\frac{\partial E}{\partial c^i_{l\alpha}} c^j_{l\alpha} + \frac{1}{2}\frac{\partial E}{\partial c^j_{l\alpha}} c^i_{l\alpha} - \mu \ddot{c}^i_{l\alpha} \dot{c}^j_{l\alpha} \right). \tag{7}$$

The total energy expression given above is modulated by a smooth cut-off function so as to permit a molecular dynamics simulation. For ground-state properties, we need to minimize the total energy (1) with respect to the ionic and the electronic coordinates. For finite-temperature simulations, the electrons are quenched to the Born–Oppenheimer surface. That is, the total energy functional is minimized with respect to the electronic coordinates at all times for a given instantaneous position of the ions, subject to the orthonormality constraints of the wave function. This is done by a self-consistent diagonalization of the Hamilton matrix. After each quenching, both the trajectories of the ionic and electronic coordinates are updated simultaneously by integrating equations (5) and (6) with the Verlet algorithm. This is repeated for N_{Born} time steps (50 in this work), after which the electrons are quenched to the Born–Oppenheimer surface again, and the procedure is repeated. During the N_{Born} steps, a 'Shake' algorithm [20] is used to impose the orthonormality constraints of equation (4) in the updating of the electronic coordinates $\{c_{l\alpha}^{j}\}$.

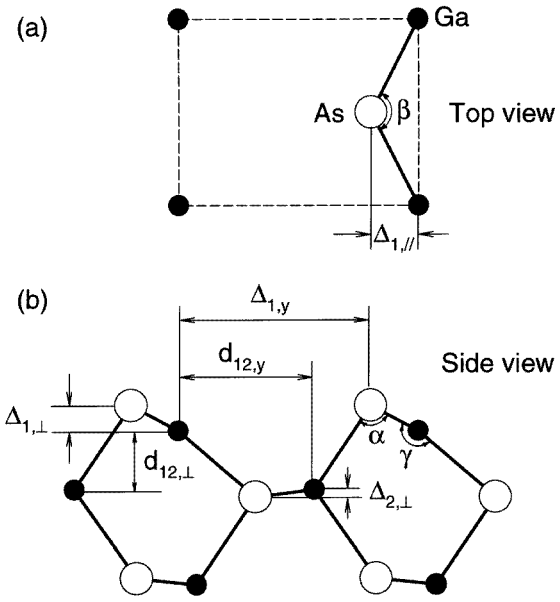

Figure 5. The atomic geometry at the GaAs(110) surface, with As atoms shown by open circles and Ga atoms by solid circles. (a) A top view of the surface unit cell. (b) A side view of the first three layers of the GaAs(110) surface.

5. The GaAs(110) surface

The GaAs(110) surface is the most thoroughly studied heteropolar semiconductor surface [21–36]. It is generally agreed that the surface does not reconstruct. Surface relaxations involve As atoms moving out of the surface and Ga atoms moving toward the bulk, as illustrated in figure 5. The atomic structure has been determined by low-energy electron diffraction (LEED) [21–25] and scanning tunnelling microscopy (STM) [26]. The latter measurements clearly show the zigzag chains of Ga and As atoms on the surface, even providing a rough measure of the surface atomic relaxations. Theoretical studies have been done with semiempirical tight-binding methods [2, 27] and self-consistent density

functional calculations [28–31]. Good agreement with the experimental measurements have been obtained in these studies. Here we use the above tight-binding formalism to determine the atomic structure of the GaAs(110) surface. Since the equilibrium structure of the GaAs(110) surface is well known, comparison with the structural results obtained using our TBMD simulation would provide an independent way of judging our method.

Our simulation cell consists of a bulk truncated slab consisting of ten atomic layers, oriented in the [110] direction, each containing four Ga atoms and four As atoms, for a total of 80 atoms. Atoms in the two middle layers are kept fixed in position to simulate the bulk. Of course, we consider the change of their electronic structure due to their interaction with atoms closer to the surface. Periodic boundary conditions are applied to simulate an infinite ten-layer slab with a (110) surface.

We start our molecular dynamics simulation with the bulk-derived geometry, with both Ga and As atoms in the same (110) plane. In this particular case, we found that heating the system is unnecessary since the potential energy of the bulk-derived geometry is high due to the strain at the surface that is associated with unsaturated dangling bonds. Consequently, the temperature of the system rises quickly when the structural constraints are lifted. This is enough for the system to sample many possible configurations, and to relax to the global minimum. After sufficient time has elapsed, we cool the system slowly to $T = 0$ K by appropriately scaling the velocities of the atoms.

Table 2. Atomic displacements from bulk-derived unrelaxed positions at the GaAs(110) surface.

	Δy (Å)		Δz (Å)	
	As	Ga	As	Ga
Surface layer	0.124	0.408	0.083	−0.508
	0.145[a]	0.399[a]	0.101[a]	−0.510[a]
	0.19[b]	0.35[b]	0.19[b]	−0.46[b]
	0.32[c]	0.48[c]	0.10[c]	−0.55[c]
Second layer	0.018	0.043	−0.079	0.097
			−0.06[b]	0.07[b]
Third layer	0.006	0.015	0.017	−0.125
			0.02[b]	−0.04[b]

[a]Reference [28].
[b]Reference [27].
[c]Reference [25].

The fully relaxed atomic structure of the topmost layers of the GaAs(110) surface is shown in figure 6. The atomic displacements and various structural parameters that have been used to describe the details of the atomic geometry of the GaAs(110) surface [21, 30, 34, 35] are summarized in tables 2, 3, and 4. Available data from previous calculations and experimental measurements are also listed in these tables for comparison. Our results for the structural parameters are generally in good agreement with the available values, as can be seen by inspection of these tables. It is noted that results obtained by Bass and Matthai [28], Hebenstreit *et al* [29], Qian *et al* [30] and Luiz *et al* [34] represent the latest first-principles calculations.

The LEED and STM results reveal that the GaAs(110) surface relaxes with the Ga atom moving inward and the As atom being displaced outward, as shown in figure 5. This well-known result is reproduced in our calculation with good accuracy. As shown in

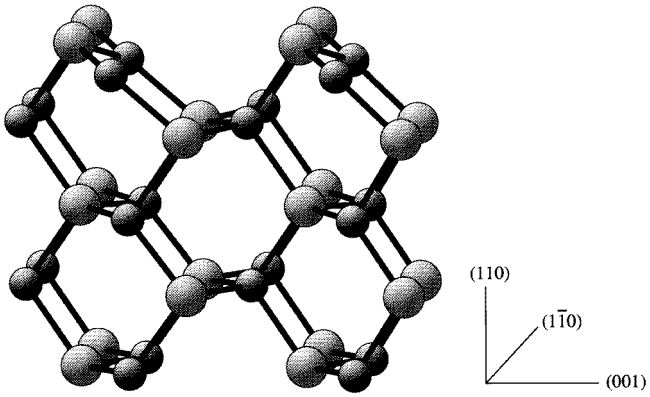

Figure 6. Fully relaxed atomic structure of the topmost few layers of the GaAs(110) surface. The As atoms are shown as the larger spheres, and the Ga atoms by the smaller spheres.

figure 6, the surface relaxes in such a way that the cations move inward to an approximately planar, threefold coordination with their anion neighbours, whereas the uppermost anions move outward into a pyramidal configuration with their three cation neighbours. Based on the interpretation in terms of the rehybridization of the surface bonds [34, 37, 38], it was predicted that the top-layer geometry lies between the bulk geometry (tetrahedral bonding)

Table 3. Changes from bulk-derived unrelaxed positions at the GaAs(110) surface, compared to other calculations and to available experimental data. The first two columns give the displacements δ of As and Ga atoms in the first layer. The buckling angle θ of the surface bond is defined by $\theta = \tan^{-1}(\Delta_{1,\perp}/\Delta_{1,\parallel})$. Other quantities are defined in figure 5. Displacements are given in Å.

Reference	As	Ga	$\Delta_{1,\perp}$	$\Delta_{2,\perp}$	$d_{12,\perp}$	$\Delta_{1,y}$	$d_{12,y}$	θ
Present	0.083	−0.508	0.592	−0.175	1.34	4.42	3.12	28.4°
Bass and Matthai [28]	0.101	−0.510						
Luiz *et al* [34]			0.67	0.098	1.415	4.407	3.190	30.2°
Hebenstreit *et al* [29]			0.63	−0.086	1.46	4.355	3.145	28.6°
Qian *et al* [30]	0.143	−0.442	0.58	−0.07	1.44	4.39	3.18	27.4°
Chadi [27]	0.186	−0.459	0.65	−0.13	1.47	4.40	3.17	27.3°
Mailhiot *et al* [35]	0.176	−0.507	0.68	0.20	1.35	4.45	3.18	29.7°
Ferraz and Srivastava [36]	0.235	−0.510	0.75	−0.035	1.46	4.45	3.36	31.6°
Meyer *et al* [21]	0.144	−0.506	0.65	−0.12	1.43	4.40	3.31	27.3°
Duke *et al* [22]	0.159	−0.527	0.686	−0.06	1.44	4.52	3.34	31.1°
Tong *et al* [23]	0.176	−0.510	0.686	−0.03	1.47	4.36	3.17	28.0°
Puga *et al* [24]	0.193	−0.515	0.708	−0.06	1.45	4.43	3.18	30.1°

Table 4. Bond angles at the anion and cation sites in the first layer.

	Present	Luiz *et al* [34]	Bulk	GaH_3	AsH_3
α	92.9°	90.0°	109.5°	—	92.1°
β	114.9°	111.7°	109.5°	—	—
γ	121.7°	123.6°	109.5°	120°	—

and the geometry obtained by putting the cation and the anion in configurations suggested by the structure of their isolated molecular hydrides, namely the planar GaH_3 molecule with 120° bond angles and the pyramidal AsH_3 molecule with bond angles of 92.1°. The bond angles α, β, and γ obtained in our simulation are listed in table 4, together with those determined by Luiz *et al* [34]. The 'pyramidal' angle α obtained in our calculation is 92.9°, and the 'planar' angle γ at the cation is 121.7°; both are closer to the isolated hydride molecule configurations than those obtained by Luiz *et al*. The value of the 'in-plane' angle β is 114.9°, compared to 111.7° obtained by Luiz *et al.* Like in other studies, there has been no atomic displacement in the $(\bar{1}10)$ direction, while in the (001) direction, the As and the Ga atoms in the surface layer move by 0.124 Å and 0.408 Å respectively, in good agreement with those obtained in other calculations. Smaller displacements in the (001) directions are also found for atoms in the second and the third layer.

The only noticeable difference between our calculated structural parameters and other results is the smaller outward relaxation of the surface As atoms (≈0.083 Å), which we relate to relatively large inward relaxations of atoms in the second and third layer. We believe that our results, based on an unrestricted structural optimization during a long simulation time, are closer to reality than those of more involved computational schemes. As mentioned above, our calculated inward relaxations for the second and the third layer are slightly larger than in other theoretical studies, such as those of reference [27], as seen in table 2. Further support for our results comes from an overall better agreement between our and others' results for the relative atomic displacements.

Based on these comparisons, we can conclude that the atomic structure obtained using our TBMD method agrees not only qualitatively, but also quantitatively very well with experimental results as well as theoretical results based on more rigorous first-principles methods. Our method can thus be used to predict surface properties of GaAs as well as other semiconductor alloys.

6. The As vacancy in GaAs

Point defects strongly affect the electrical and optical properties of semiconductors. Since they are elemental native defects in GaAs, As vacancies in various charge states have been studied by a number of authors [15, 39–47]. Most of these studies, with the notable exceptions of references [15] and [44], are concerned only with the electronic structure at the defect site, and neglect ionic relaxation.

According to Laasonen *et al* [44], the relaxation of neighbours of a given defect can be described in terms of three displacement components: the 'breathing' mode, which gives the radial relaxation (inward or outward) of an ion, and two 'pairing' modes, which measure the lateral displacements of the ions (i.e., perpendicular to the breathing mode). Using *ab initio* molecular dynamics, Laasonen *et al* [44] obtained a small (2–3%) outward relaxation, and an even smaller (0.6%) pairing-mode relaxation for the neutral As vacancy in GaAs. A larger breathing-mode displacement was obtained by Seong and Lewis [15] using tight-binding molecular dynamics developed by Molteni *et al* [12–14]. However, the local tetrahedral symmetry was broken, as one neighbour atom of the defect relaxed inward while the other three relaxed outward. These authors also found that the pairing-mode relaxations are very small.

Here we present a simulation study of the As vacancy in GaAs using our newly developed TBMD method, and compare our results with those obtained in references [15] and [44]. Our simulations were carried out using a 64-atom supercell, from which a single As atom was removed in order to study the vacancy. Periodic boundary conditions in all

three Cartesian directions were used to eliminate surface effects. The ground-state structure was determined by performing a full, unconstrained relaxation of the atomic positions.

Table 5. Displacements in Å of Ga atoms that are nearest neighbours to the As vacancy in GaAs.

Atom	Δx	Δy	Δz	Δr
1	−0.23	−0.30	−0.23	0.45
2	−0.23	0.23	0.30	0.45
3	0.30	0.23	−0.23	0.45
4	−0.38	0.38	−0.38	0.65

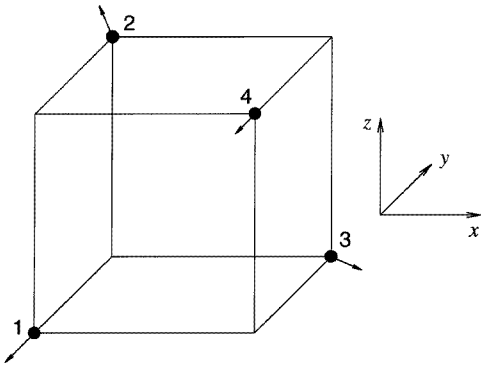

Figure 7. Relaxations of the Ga atoms that are nearest neighbours of the As vacancy in GaAs. The arrows indicate the direction and magnitude of displacement for each atom.

The distortions of the four Ga nearest neighbours of the As vacancy, obtained in our TBMD study, are listed in table 5 and also shown schematically in figure 7, where the arrows indicate the directions and magnitudes of atomic relaxations. In agreement with the TBMD results obtained by Seong and Lewis [15], we found that three of the Ga neighbours of the As vacancy relax outward, while the other Ga atom relaxes inward, leading to a trigonal distortion with a C_{3v} symmetry. The magnitudes of the atomic displacements obtained in our study are also in good agreement with those obtained by Seong and Lewis.

Table 6. Orbital populations in electron charges of Ga atoms that are nearest neighbours to the As vacancy in GaAs.

Atom	s	p_x	p_y	p_z	Total charge
1	1.39	0.55	0.55	0.55	3.04
2	1.39	0.55	0.55	0.55	3.04
3	1.39	0.55	0.55	0.55	3.04
4	1.92	0.45	0.45	0.45	3.28

The electronic structure of a vacancy in a III–V semiconductor is now well established. It is mainly characterized by two states with a_1 and t_2 symmetry which can be in the forbidden band gap. The t_2 state is triply degenerate, while the a_1 state is non-degenerate.

For the neutral As vacancy, the a_1 and t_2 states are populated by two and one electrons, respectively. A Jahn–Teller distortion splits the t_2 state into a lower-lying non-degenerate component which becomes occupied, and an upper doubly degenerate state that remains empty. The Jahn–Teller distortion can be tetragonal or trigonal [48, 49]. The atomic displacements obtained in our TBMD study, as well as those obtained by Seong and Lewis, show clearly a trigonal distortion with a C_{3v} symmetry. This is in contrast to the results obtained by Laasonen *et al* [44] based on *ab initio* molecular dynamics, which show a tetragonal distortion with the D_{2d} symmetry. Furthermore, in the case of a tetragonal distortion, the electron is localized on the four neighbours, whereas for a trigonal distortion the electron resides mainly on only one neighbour [46]. The calculated orbital population at the four Ga sites that are nearest neighbours of the As vacancy are listed in table 6. It is clear that the atom with the largest inward relaxation acquires the largest charge. Compared to the other three Ga nearest neighbours of the vacancy, the charge distribution on this Ga atom is less polarized, with almost two electrons in the s orbital and a relatively small charge populating the p orbitals. This Ga atom thus forms weaker and longer bonds with the next-nearest-neighbour As atoms.

It is interesting to note that at early stages of our TBMD simulation, the relaxations of the Ga atoms that are nearest neighbours of the vacancy were symmetric, with all four atoms relaxing outward. However, as the simulation continued, one of these Ga neighbours started to relax inward, causing the trigonal distortion and further reductions in total energy of the system. We also note that the magnitudes of the atomic relaxations obtained in the present study and also in the TBMD study by Seong and Lewis are nearly one order of magnitude larger than those obtained by Laasonen *et al*. It is therefore reasonable to believe that the tetragonal distortion obtained by Laasonen *et al* could correspond to a metastable state, as simulation times in *ab initio* molecular dynamics are typically short and possibly insufficient for determining the true equilibrium state. The reasons mentioned above make us believe that the trigonal distortion obtained in the TBMD studies should represent the true equilibrium geometry. While both distortions are in principle possible, further rigorous total energy calculation is required to determine which structure is more stable.

7. GaAs clusters

Structural and electronic properties of small atomic clusters have been a subject of great interest for both experimental and theoretical studies. Most of these studies, however, focus on clusters formed from a single element. Theoretical studies on compound clusters formed from two or more elements have been limited due to computational difficulties arising from the large number of structural and permutational isomers formed due to multiple elements. A number of theoretical [50–66] and experimental [67, 68] attempts have been made to determine the structure and properties of small Ga_mAs_n clusters. The electronic and geometric structures of Ga_nAs_n ($1 \leqslant n \leqslant 4$) clusters have been studied by Song *et al* [50] using *ab initio* molecular orbital theory (MOT). Andreoni [51] also studied the equilibrium structure of the Ga_nAs_n clusters for $n = 2$–5 as well as their stability and thermal behaviour using the Car–Parrinello (CP) method. Lou *et al* [52] calculated the electronic and geometrical structures of both stoichiometric and non-stoichiometric small Ga_mAs_n clusters ($m + n \leqslant 10$) using the local spin-density functional method (LSDF) and found that even-numbered clusters are closed-shell systems with a singlet ground state, whereas odd-numbered clusters are open-shell systems. Al-Laham and Raghavachari [53] studied the electronic structure and stability of Ga_nAs_n clusters for $n = 1$–3 using the effective core potential (ECP) and found that Ga_3As_3 has a capped trigonal bipyramid

ground-state structure, and that the electronegativity difference between the constituents of a mixed cluster plays a major role in electronic structure properties. Much work has been done by Graves and Scuseria to investigate ground-state properties of small Ga_mAs_n clusters using self-consistent-field theory (SCF) and coupled-cluster theory (CCSD) [54–57]. Small Ga_mAs_n clusters were also studied by Meier *et al* [58] using *ab initio* multi-reference single and double excitation configuration interaction method (MRD-CI), and extensively by Balasubramanian [59–65] using relativistic *ab initio* complete-active-space self-consistent-field (CASSCF) theory, and large-scale configuration interaction calculations. More recently, Buda and Fasolino studied the stability and optical properties of small III–V hydrogenated clusters using an *ab initio* molecular dynamics method [66].

On the experimental side, Lemire *et al* [67] obtained the spectrum of Ga_1As_1 by resonant two-phonon ionization spectroscopy. The ground state was identified as $^3\Sigma^-$, derived from a $\sigma^2\pi^2$ molecular configuration. The bond length was found to be 2.53 ± 0.02 Å and the ionization potential was 7.17 ± 0.75 eV, with a binding energy of 2.06 ± 0.05 eV. Very recently, the static polarizabilities of isolated GaAs clusters have been investigated as a function of cluster size and temperature by Schäfer *et al* [68].

In this study, we use our semiempirical, bulk-fitted, TB total energy scheme to determine the structures of small Ga_mAs_n clusters. Our results for Ga_mAs_n clusters with $2 \leqslant m+n \leqslant 4$, that are presented here, are compared with results of other calculations.

Balasubramanian [62] has enumerated possible isomers of Ga_mAs_n clusters containing up to ten atoms. The number of possible atomic arrangements of a cluster increases rapidly with cluster size. In order to find the equilibrium structure, we start with many possible configurations, some of them suggested by Balasubramanian, and use TBMD to relax these structures until a minimum of the total energy is found. The equilibrium structure was chosen as the structure with the lowest energy.

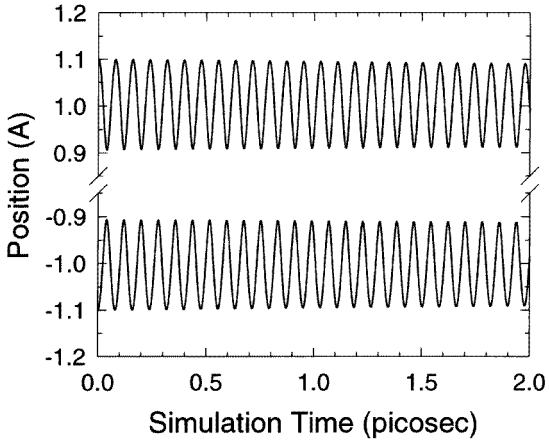

Figure 8. The time dependence of the atomic positions in the As_2 dimer along the bond length. The time step used in the simulation was $1.018\,05 \times 10^{-17}$ s. The atoms are shown to perform a harmonic oscillation with a period of 7.915×10^{14} s. The equilibrium bond length is 2.02 Å.

In figure 8, we show the positions of the two As atoms of the As_2 dimer as functions of simulation time. For a starting bond length close to the equilibrium value, the atoms perform simple harmonic oscillations, with a period of 7.915×10^{-14} s, which corresponds to an oscillation frequency of 421 cm^{-1} in this case. Similar behaviour is observed for the Ga_2 and the Ga_1As_1 dimers. The calculated equilibrium bond lengths, binding energies, and

Table 7. Equilibrium properties of dimers Ga_1As_1, As_2, and Ga_2. d is the equilibrium separation of the atoms, E_b is the binding energy per atom, and ω is the vibrational frequency.

Method	d (Å)	E_b (eV)	ω (cm^{-1})	Reference
Ga_1As_1				
TBMD	2.39	2.08	254	Present work
Experiment	2.53	2.06	215	[67]
LSDF	2.55	2.46	216	[52]
SCF	2.58	0.84	210	[54, 55]
CASSCF	2.65	1.24	187	[61, 62, 63, 64]
MRD-CI	2.65	1.35		[58]
MOT	2.42	1.53		[50]
ECP	2.62	1.49		[53]
CCSD	2.56	1.84	217	[55]
As_2				
TBMD	2.02	4.0	421	Present work
Experiment	2.103	3.96	430	[69]
LSDF	2.11	4.77	427	[52]
SCF	2.059		514	[57]
CCSD	2.107		447	[57]
CASSCF	2.164	2.71	394	[60]
Ga_2				
TBMD	2.68	1.76	311	Present work
LSDF	2.716	1.74		[52]
SCF	2.762		162	[56]
CCSD	2.715		169	[56]
CASSCF	2.762		158	[59]

oscillation frequencies are summarized in table 7. The experimental and other theoretical values are also listed for comparison. We find our TBMD results to be generally in fair agreement with other values. The only exception is our value of the Ga_2 oscillation frequency, which is twice as high as other calculated values; no experimental data are available for this quantity.

Table 8. Ground-state geometries of the trimers Ga_1As_2 and Ga_2As_1. d(A–B) (where A, B are Ga or As) is the equilibrium separation in Å between the atoms A and B. θ(A–B–C), given in degrees, is the angle formed by the bonds B–A and B–C. E_b is the binding energy per atom in eV.

Ga_1As_2					
Method	d(Ga–As)	d(As–As)	θ(As–Ga–As)	E_b	Reference
TBMD	2.65	2.11	47.1	3.49	Present work
LSDF	2.73	2.20	47.5	2.31	[52]
CASSCF	2.85	2.21	45.5		[63]
MRD-CI	2.87	2.27	46.6		[58]
Ga_2As_1					
Method	d(Ga–As)	d(Ga–Ga)	θ(Ga–As–Ga)	E_b	Reference
TBMD	2.43/2.31	3.56	94.7	2.75	Present work
LSDF	2.33	3.52	98.0	1.93	[52]

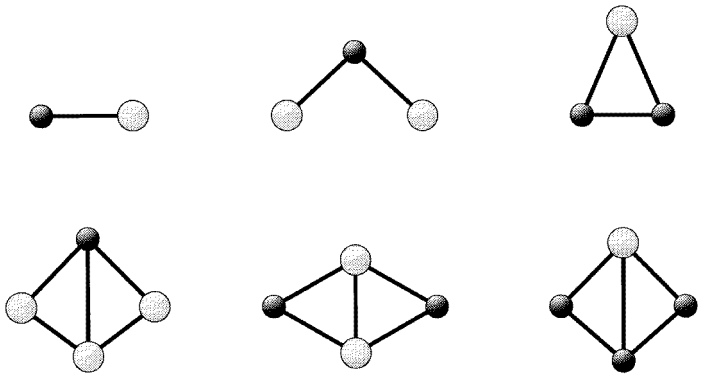

Figure 9. Ground-state geometries of small semiconductor alloy clusters: GaAs, $GaAs_2$, Ga_2As, $GaAs_3$, Ga_2As_2, and Ga_3As. The As atoms are shown by the larger light spheres, and the Ga atoms by the smaller dark spheres.

Table 9. Ground-state geometries of the tetramers Ga_1As_3, Ga_3As_1, and Ga_2As_2. d(A–B) (where A, B are Ga or As) is the equilibrium separation in Å between atoms A and B. θ(A–B–C), given in degrees, is the angle formed by the bonds B–A and B–C. E_b is the binding energy per atom in eV.

Ga_1As_3					
Method	d(Ga–As)	d(As–As)	θ(Ga–As–As)	E_b	Reference
TBMD	2.49	2.30	69.4	3.84	Present work
LSDF	2.39	2.34	66.9	2.66	[52]
Ga_3As_1					
Method	d(Ga–As)	d(Ga–Ga)	θ(As–Ga–Ga)	E_b	Reference
TBMD	2.31	2.17	83.4	3.44	Present work
LSDF	2.37	2.50	78.1	2.38	[52]
Ga_2As_2					
Method	d(As–As)	d(As–Ga)	θ(As–Ga–As)	E_b	Reference
TBMD	2.43	2.46	59	3.60	Present work
MOT	2.28	2.71		1.83	[50]
CP			52		[51]
LSDF	2.40	2.70		2.22	[52]
ECP	2.29	2.71		2.48	[53]
SCF	2.28	2.70	49.8	0.84	[54]
CASSCF	2.30	2.68	50.3	1.88	[63]
MRD-CI	2.38	2.74	51.2		[58]

For the Ga_2As_1 and Ga_1As_2 trimers, there are three possible stable structures: the symmetric and asymmetric linear structures, and the triangular structures in each case. Using the local spin-density functional technique, Lou *et al* [52] found that the equilibrium geometries are bent, as shown in figure 9. Our TBMD simulation results also show that the triangular structures are the most stable in each case. The bond lengths and bond angles obtained are listed in table 8. In Ga_1As_2, the bond angle is 47.1°, and in Ga_2As_1, the angle is 94.7°. The small bond angle in Ga_1As_2 is due to the short As–As bond length of 2.11 Å. The larger bond angle in Ga_2As_1 is a consequence of a weak Ga–Ga bond and relatively

strong Ga–As bonds. For the linear forms, we found that the chain with a terminal Ga atom is more stable than one with Ga in the centre for Ga_1As_2. For Ga_2As_1, on the other hand, the isomer with As in the middle was found to be more stable than that with a terminal As atom, also in agreement with Lou *et al*.

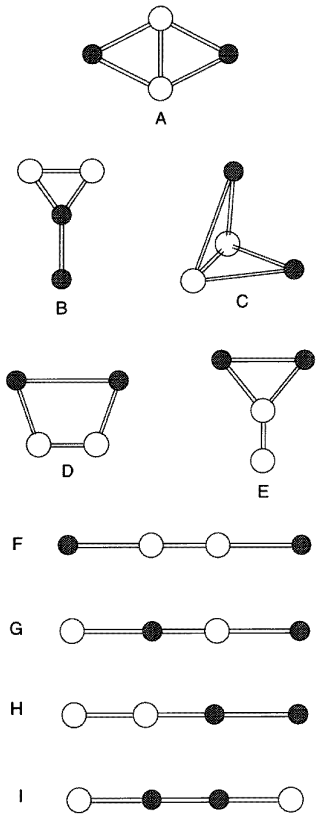

Figure 10. Possible stable geometries of Ga_2As_2. The As atoms are shown by the larger white spheres, and the Ga atoms by the smaller dark spheres.

As shown in figure 10, there are several possible stable structures for Ga_2As_2. Using *ab initio* molecular orbital theory, Song *et al* [50] has calculated the binding energy for each of the nine possible structures and found that the ground state is the planar rhombus, in agreement with other studies. Our TBMD study also found that the planar rhombus structure is the most stable one with a binding energy of 3.60 eV per atom. The bond lengths and bond angles obtained by different theoretical methods are in good agreement, as shown in table 9. Also in agreement with results obtained by Song *et al*, we found the linear structures to be the least stable ones, with much weaker bonding. The other non-linear structures have binding energy values that are very close to each other, yet lower than those of the linear structures and higher than that of the rhombus. The symmetric linear structure with two Ga atoms at the centre (I), which Song *et al* predicted to be the least stable geometry of the Ga_2As_2 cluster, and the tetrahedron structure (C), which is the only possible three-dimensional structure, were both found to be unstable in our study, the latter gradually transforming into a rhombus after sufficient simulation time.

Lou *et al* [52] have also studied the non-stoichiometric Ga_1As_3 and Ga_3As_1 clusters using the local spin-density functional method. They found the C_{2v} planar structures, shown in figure 9, to represent the equilibrium geometries. In our TBMD study, a number of

possible atomic arrangements were optimized until a minimum of the total energy was found. The associated structure is believed to be the equilibrium structure. In agreement with Lou *et al* we also found the ground-state geometries to be planar. Our results, summarized in table 9, show that our bond lengths and bond angles are in reasonable agreement with those found by Lou *et al* using the local spin-density functional method.

Quite often, a tight-binding parametrization of first-principles electronic structure or experimental results depends on the crystal structure selected, and parameters obtained for one system are not necessarily transferable to other systems. The success of our tight-binding total energy scheme in predicting ground-state properties of small Ga_mAs_n clusters, however, shows that our parameters, based on bulk systems, are widely transferable to systems as different from the bulk as small clusters. Similar results, that we obtained for larger Ga_mAs_n and also AlAs clusters, confirm this conclusion, and will be published separately. We believe that our approach has been proven reliable for predicting ground-state structural properties of alloy semiconductor clusters, in particular the relative stability of individual isomers and the size dependence of the binding energy.

8. Conclusions

A tight-binding molecular dynamics method has been developed to determine electronic and structural properties of heterovalent semiconductor compounds. Structure-independent parametrization has been obtained by fitting *ab initio* band structures and total energies of bulk compounds with different structures and lattice parameters. Applications of this method to the GaAs(110) surface, the As vacancy in GaAs, and small GaAs clusters yield results in agreement with available data for a fraction of the computational effort associated with *ab initio* techniques.

The calculated equilibrium structure of the GaAs(110) surface shows excellent agreement with available data. Using this method, a trigonal Jahn–Teller distortion has been predicted to occur near a neutral As vacancy in bulk GaAs. This result agrees with a similar prediction of Seong and Lewis [15], but contradicts results obtained using *ab initio* molecular dynamics that suggest a tetragonal distortion. Based on the dynamical evolution of the vacancy system, observed in our simulation, the trigonal distortion appears to be energetically more favourable. Further calculations are required to determine the relative stability of these two kinds of Jahn–Teller distortion.

The newly developed TBMD method is also able to predict the relative stability of GaAs clusters. In all of the cases considered in this study, the correct ground-state geometries were predicted by the TBMD calculation with reasonable accuracy. For various isomers of the same size and composition, the TBMD method was able to determine the correct relative stability. The low computational effort associated with our approach bears promise to as regards performing extensive ‘quantum mechanical’ molecular dynamics simulations for heterovalent compound semiconductors using the present method, in order to investigate their behaviour in the bulk, at the surface, in clusters, or near atomic defects.

Acknowledgments

One of us (DT) acknowledges the hospitality of the Theoretical Physics group at the National University of Singapore, where most of this research was performed, and partial financial support from the National Science Foundation under Grant Number PHY-92-24745 and the Office of Naval Research under Grant Number N00014-90-J-1396.

References

[1] Hohenberg P and Kohn W 1964 *Phys. Rev.* **136** B864
Kohn W and Sham L J 1965 *Phys. Rev.* **140** A1133
[2] Chadi D J 1984 *Phys. Rev.* B **29** 85 and references therein.
[3] Tománek D and Schlüter M A 1986 *Phys. Rev. Lett.* **56** 1055
Tománek D and Schlüter M A 1987 *Phys. Rev.* B **36** 1208
Alerhand O L and Mele E J 1987 *Phys. Rev.* B **35** 5533
[4] Khan F S and Broughton J Q 1989 *Phys. Rev.* B **39** 3688
[5] Wang C Z, Chan C T and Ho K M 1989 *Phys. Rev.* B **39** 8592
[6] Goodwin L, Skinner A J and Pettifor D G 1989 *Europhys. Lett.* **9** 701
[7] Laasonen K and Nieminen R M 1990 *J. Phys.: Condens. Matter* **2** 1509
[8] Lim H S, Low K C and Ong C K 1993 *Phys. Rev.* B **48** 1595
[9] Low K C and Ong C K 1994 *Phys. Rev.* B **50** 5352
[10] Feng Y P, Wee T H, Ong C K and Poon H C 1996 *Phys. Rev.* B **54** 4766
[11] Wee T H, Feng Y P, Ong C K and Poon H C 1996 *J. Phys.: Condens. Matter* **8** 6511
[12] Molteni C, Colombo L and Miglio L 1994 *J. Phys.: Condens. Matter* **6** 5243
Molteni C, Colombo L and Miglio L 1994 *J. Phys.: Condens. Matter* **6** 5255
[13] Molteni C, Colombo L and Miglio L 1993 *Europhys. Lett.* **24** 659
[14] Molteni C, Colombo L and Miglio L 1994 *Phys. Rev.* B **50** 4371
[15] Seong H and Lewis L J 1995 *Phys. Rev.* B **52** 5675
[16] Seong H and Lewis L J 1996 *Phys. Rev.* B **53** 4408
[17] Slater J C and Koster G F 1954 *Phys. Rev.* **94** 1498
[18] Harrison W A 1989 *Electronic Structure and the Properties of Solids: The Physics of the Chemical Bond* (New York: Dover)
[19] Car R and Parrinello M 1985 *Phys. Rev. Lett.* **55** 2471
[20] Rychaert J P, Ciccotti G and Berendsen H J C 1977 *J. Comput. Phys.* **23** 327
[21] Meyer R J, Duke C B, Paton A, Kahn A, So E, Yeh J L and Mark P 1979 *Phys. Rev.* B **19** 5194
[22] Duke C B, Richardson S L, Paton A and Kahn A 1983 *Surf. Sci.* **127** L135
[23] Tong S Y, Mei W N and Xu G 1984 *J. Vac. Sci. Technol.* B **2** 393
[24] Puga M W, Xu G and Tong S Y 1985 *Surf. Sci.* **164** L789
[25] Tong S Y, Lubinsky A R, Mrstik B J and Van Hove M A 1978 *Phys. Rev.* B **17** 3303
[26] Feenstra R M and Fein A P 1985 *Phys. Rev.* B **32** 1394
Feenstra R M, Stroscio J A, Tersoff J and Fein A P 1987 *Phys. Rev. Lett.* **58** 1192
Feenstra R M 1994 *Phys. Rev.* B **50** 4561
[27] Chadi D J 1979 *Phys. Rev.* B **19** 2074
Chadi D J 1978 *Phys. Rev.* B **18** 1800
[28] Bass J M and Matthai C C 1995 *Phys. Rev.* B **52** 4712
[29] Hebenstreit J, Heinemann M and Scheffler M 1991 *Phys. Rev. Lett.* **67** 1031
[30] Qian G X, Martin R M and Chadi D J 1988 *Phys. Rev.* B **37** 1303
[31] Pandey K C 1982 *Phys. Rev. Lett.* **49** 223
[32] Faul J, Neuhold G, Ley L, Fraxedas J, Zollner S, Riley J D and Leckey R C G 1993 *Phys. Rev.* B **47** 12 625
[33] Beres R P and Allen R E 1983 *Solid State Commun.* **45** 13
[34] Luiz J, Alves A, Hebenstreit J and Scheffler M 1991 *Phys. Rev.* B **44** 6188
[35] Mailhiot C, Duke C B and Chadi D J 1985 *Surf. Sci.* **149** 366
[36] Ferraz A C and Srivastava G P 1987 *Surf. Sci.* **182** 161
[37] Lubinsky A R, Duke C B, Lee B W and Mark P 1976 *Phys. Rev. Lett.* **36** 1058
Duke C B, Lubinsky A R, Lee B W and Mark P 1976 *J. Vac. Sci. Technol.* **13** 761
Kahn A 1983 *Surf. Sci. Rep.* **3** 193
[38] Swarts C A, Goddard W A III and McGill T C 1980 *J. Vac. Sci. Technol.* **17** 982
Swarts C A, McGill T C and Goddard W A III 1981 *Surf. Sci.* **110** 400
[39] Scheffler M and Scherz U 1986 *Proc. 14th Int. Conf. on Defects in Semiconductors (Paris, 1986); Mater. Sci. Forum* **10–12** 353
[40] Puska M J 1989 *J. Phys.: Condens. Matter* **1** 7347
[41] Puska M J, Jepsen O, Gunnarsson O and Nieminen R M 1986 *Phys. Rev.* B **34** 2695
[42] Jansen R W and Sankey O F 1989 *Phys. Rev.* B **39** 3192
[43] Zhang S B and Northrup J E 1991 *Phys. Rev. Lett.* **67** 2339
[44] Laasonen K, Nieminen R M and Puska J J 1992 *Phys. Rev.* B **45** 4122

[45] Gilgien L, Galli G, Gygi F and Car R 1994 *Phys. Rev. Lett.* **72** 3214
[46] Delerue C 1991 *Phys. Rev.* B **44** 10 525
[47] Bachelet G B, Baraff G A and Schlüter M 1981 *Phys. Rev.* B **24** 915
[48] Lannoo M and Bourgoin J 1981 *Point Defects in Semiconductors I (Springer Series in Solid State Sciences 22)* (Berlin: Springer)
Bourgoin J and Lannoo M 1983 *Point Defects in Semiconductors II (Springer Series in Solid State Sciences 35)* (Berlin: Springer)
[49] Watkins G D 1973 *Radiation Damage and Defects in Semiconductors (Reading, 1972) (Inst. Phys. Conf. Ser. 7)* ed J E Whitehouse (Bristol: Institute of Physics Publishing) p 228
[50] Song K M, Ray A K and Khowash P K 1994 *J. Phys. B: At. Mol. Phys.* **27** 1637
[51] Andreoni W 1992 *Phys. Rev.* B **45** 4203
[52] Lou L, Nordlander P and Smalley R E 1992 *J. Chem. Phys.* **97** 1858
Lou L, Wang L, Chibante L P F, Laaksonen R T, Nordlander P and Smalley R E 1991 *J. Chem. Phys.* **94** 8015
[53] Al-Laham M A and Raghavachari K 1991 *Chem. Phys. Lett.* **187** 13
Raghavachari K and Al-Laham M A 1992 *Physics and Chemistry of Finite Systems: From Clusters to Crystals* vol I, ed P Jena *et al* (Dordrecht: Kluwer Academic) pp 639–44
[54] Graves R M and Scuseria G E 1991 *J. Chem. Phys.* **95** 6602
[55] Scuseria G E 1991 *Theor. Chim. Acta* **80** 215
[56] Graves R M and Scuseria G E, unpublished
[57] Scuseria G E 1990 *J. Chem. Phys.* **92** 6722
[58] Meier U, Peyerimhoff S D and Grein F 1991 *Chem. Phys.* **150** 331
[59] Balasubramanian K 1986 *J. Phys. Chem.* **90** 6786
[60] Balasubramanian K 1987 *J. Mol. Spectrosc.* **121** 465
[61] Balasubramanian K 1987 *J. Chem. Phys.* **86** 3410
[62] Balasubramanian K 1988 *Chem. Phys. Lett.* **150** 71
[63] Balasubramanian K 1990 *Chem. Phys. Lett.* **171** 58
[64] Balasubramanian K 1990 *J. Mol. Spectrosc.* **139** 405
[65] Balasubramanian K 1990 *Chem. Rev.* **90** 93
[66] Buda F and Fasolino A 1995 *Phys. Rev.* B **52** 5851
[67] Lemire G W, Bishea G A, Heidecke S A and Morse M D 1990 *J. Chem. Phys.* **92** 121
[68] Schäfer R, Schlecht S, Woenckhaus J and Becker J A 1996 *Phys. Rev. Lett.* **76** 471
[69] Huber K P and Herzberg G 1979 *Constants of Diatomic Molecules* (New York: Van Nostrand)